Proceedings of the
47th IEEE Conference on Decision and Control
Cancun, Mexico, Dec. 9-11, 2008

A Nonlinear GPS/IMU Based Observer for Rigid Body Attitude and Position Estimation

J.F. Vasconcelos, C. Silvestre and P. Oliveira

Abstract— **This work proposes a position and attitude nonlinear observer based on inertial measurements and GPS pseudorange readings. The observation problem is formulated on $\mathrm{SE}(3)$, and the solution yields exponential convergence of the attitude and position estimates. The GPS pseudorange measurements and inertial sensor readings are exploited directly in the observer, and the integration of vector readings in the observer is discussed. The proposed observer dynamics compensate for the bias in the angular velocity sensor and the clock offset in GPS pseudorange measurements. The stability of the position and velocity estimates in the presence of bounded accelerometer noise is also analyzed. The properties of the GPS/IMU based observer are illustrated in simulation for a rigid body describing a challenging trajectory.**

I. INTRODUCTION

Navigation systems that integrate Inertial Measurement Unit (IMU) with Global Positioning Satellite (GPS) data have become a widely adopted solution for practical applications over the last decades [11]. The IMU comprises rate gyro and accelerometer triads, rigidly mounted on the vehicle structure (strapdown configuration). Using the data provided by these sensors, high-accuracy algorithms compute attitude, velocity and position. Non-ideal characteristics of the inertial sensors, namely bias, misalignment, and noise, degrade the results of the integration algorithm and produce medium-term drift of the position and attitude estimates. The GPS receiver, installed onboard the vehicle, is a position aiding system that provides pseudorange measurements with respect to satellites in view. Algorithms to compute the position of the GPS receiver in Earth frame using the pseudorange measurements are presented in [2], [4], [6], [8], [15].

The integration of the short-term high-accuracy IMU data with the GPS unit readings allows for improved position and attitude estimates. To that effect, Kalman and sigma-point filtering techniques are commonly adopted [11], [10], [21], which, by means of linearization, dynamically compensate for the estimation errors of the IMU/GPS ensemble. Due to the inherently nonlinear attitude kinematics, the stability and robustness of the IMU/GPS filtering architectures are validated using experimental data.

The authors are with the Institute for Systems and Robotics (ISR), Instituto Superior Técnico, Lisbon, Portugal. E-mails: {jfvasconcelos, cjs, pjcro}@isr.ist.utl.pt
Tel: (+351) 21-8418054, Fax: (+351) 21-8418291.

This work was partially supported by Fundação para a Ciência e a Tecnologia (ISR/IST plurianual funding) through the POS Conhecimento Program that includes FEDER funds and by the project PTDC/EEA-ACR/72853/2006 HELICIM. The work of J.F. Vasconcelos was supported by a PhD Student Scholarship, SFRH/BD/18954/2004, from the Portuguese FCT POCTI programme.

More recently, nonlinear observers have been proposed for the problems of attitude and position determination [3], [12], [14], [18], [19], [22], [23], formulated rigorously in non-Euclidean spaces where attitude is naturally represented, such as the set of rotation matrices $\mathrm{SO}(3)$ and the set of unit quaternions $\mathrm{S}(3)$. Insights on the problem of nonlinear attitude estimation and theoretical stability and convergence results are brought about in this approach. Guidelines for observer design on manifolds such as $\mathrm{SO}(3)$ and $\mathrm{S}(3)$ and the topological issues arising in global stabilization on non-Euclidean spaces are evidenced in [5], [9].

In this work, a GPS/IMU based nonlinear observer is proposed, characterized by a cascaded composition of the attitude observer with the position observer. Exploiting inertial measurements and pseudorange readings directly, the observer is formulated on $\mathrm{SE}(3)$ and yields exponential convergence of the position and attitude estimation errors to the origin. Non-ideal characteristics of the inertial sensors are addressed. Rate gyro bias is compensated dynamically and the position and velocity errors are stabilized in the presence of accelerometer noise. The proposed attitude observer exploits IMU readings, aided by vector measurements as presented in previous work by the authors [23], or by using multiple GPS receivers installed onboard the vehicle, allowing for an observer based solely on GPS and IMU data. Convergence bounds for the estimation errors flow from the stability proofs and from the recently derived results for parameterized linear time-varying systems [16].

The paper is organized as follows. In Section II, the sensor suite adopted in the estimation problem is described and Section III proposes attitude and position observers based on the GPS, IMU and vector readings. The stability and convergence properties of the estimation errors are derived and the observer equations are expressed as explicit functions of the sensor measurements. The stability and convergence of the observer estimates are illustrated in simulation in Section IV. Concluding remarks are presented in Section V.

NOMENCLATURE

The notation adopted is fairly standard. The set of $n \times m$ matrices with real entries is denoted as $\mathrm{M}(n, m)$ and $\mathrm{M}(n) := \mathrm{M}(n, n)$. The set of special orthogonal matrices is denoted as $\mathrm{SO}(n) := \{\mathbf{R} \in \mathrm{M}(n) : \mathbf{R}'\mathbf{R} = \mathbf{I}, \det(\mathbf{R}) = 1\}$, the special Euclidean group is given by the product space $\mathrm{SE}(n) := \mathrm{SO}(n) \times \mathbb{R}^n$ [17], and the n-dimensional sphere is described by $\mathrm{S}(n) := \{\mathbf{x} \in \mathbb{R}^{n+1} : \mathbf{x}'\mathbf{x} = 1\}$. The time dependence of the variables will be omitted in general, but otherwise denoted for the sake of clarity.

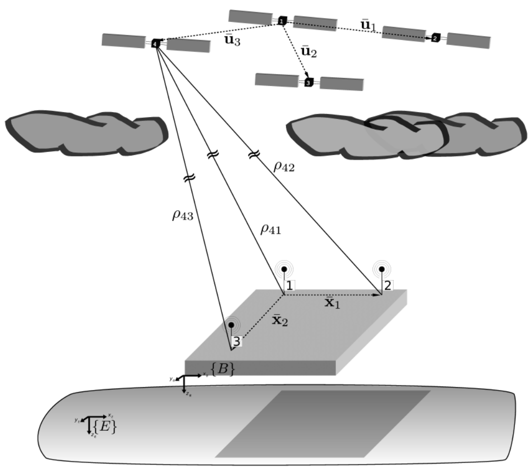

Fig. 1. Navigation System Configuration

II. SENSOR DESCRIPTION

In this section, the sensor suite used in the attitude and position observer is introduced. The rigid body kinematics are described by

$$\dot{\bar{\mathcal{R}}} = \bar{\mathcal{R}}(\bar{\boldsymbol{\omega}})_\times, \quad {}^E\dot{\bar{\mathbf{p}}} = {}^E\bar{\mathbf{v}}, \quad {}^E\dot{\bar{\mathbf{v}}} = {}^E\bar{\mathbf{a}},$$

where $\bar{\mathcal{R}}$ is the shorthand notation for the rotation matrix ${}^E_B\mathbf{R}$ from body frame $\{B\}$ to Earth frame $\{E\}$ coordinates, $\bar{\boldsymbol{\omega}}$ is the body angular velocity expressed in $\{B\}$, ${}^E\bar{\mathbf{p}}$, ${}^E\bar{\mathbf{v}}$ and ${}^E\bar{\mathbf{a}}$ are the position, velocity and acceleration of the rigid body with respect to $\{E\}$ expressed in $\{E\}$, respectively, and $(\mathbf{s})_\times$ is the skew symmetric matrix defined by the vector $\mathbf{s} \in \mathbb{R}^3$ such that $(\mathbf{s})_\times \mathbf{b} = \mathbf{s} \times \mathbf{b}$, $\mathbf{b} \in \mathbb{R}^3$.

The inertial sensors measure the angular velocity and specific force of the body, which allows for the propagation of the attitude and position in time. The body angular velocity is measured by a rate gyro sensor triad, corrupted by a bias term

$$\boldsymbol{\omega}_r = \bar{\boldsymbol{\omega}} + \bar{\mathbf{b}}_\omega, \tag{1}$$

where the nominal bias is considered constant, $\dot{\bar{\mathbf{b}}}_\omega = \mathbf{0}$. The triaxial accelerometer measures the specific force, which is the difference between the inertial and the gravitational accelerations of the rigid body [7], ${}^B\bar{\mathbf{a}}$ and ${}^B\bar{\mathbf{g}}$ respectively, expressed in body frame coordinates,

$$\mathbf{a}_r = {}^B\bar{\mathbf{a}} - {}^B\bar{\mathbf{g}}. \tag{2}$$

The GPS pseudoranges measurements are given by the distance from the GPS satellites to the receiver and a distance offset due to the clock bias [11], yielding

$$\rho_{ij} = \|{}^E\bar{\mathbf{p}}_j - {}^E\bar{\mathbf{p}}_{S\,i}\| + b_c, \tag{3}$$

where ${}^E\bar{\mathbf{p}}_j$ and ${}^E\bar{\mathbf{p}}_{Si}$ are the positions of the receiver j and satellite i expressed in $\{E\}$, the total number of GPS satellites and receivers are represented by s and r, respectively, $j = 1..r$ and $i = 1..s$, and b_c is the range bias due to the offset between the receiver and satellite's clocks. In the communication process, the satellite coordinates ${}^E\bar{\mathbf{p}}_{Si}$ are transmitted to the receiver. Without loss of generality, receiver 1 is considered to be at the origin of the body frame, i.e. ${}^E\bar{\mathbf{p}} = {}^E\bar{\mathbf{p}}_1$.

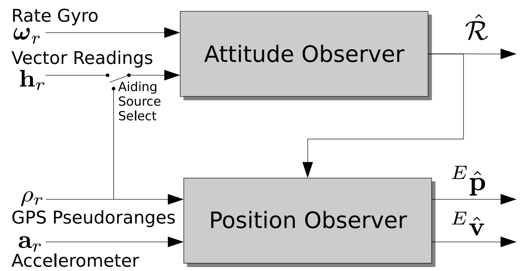

Fig. 2. Cascaded Position and Attitude Observer

The objective of the present work is to exploit the information provided by the sensors, by deriving a position and attitude observer that combines the inertial measurements with the pseudorange readings and, if available, with the vector observations.

III. OBSERVER ARCHITECTURE

As depicted in Fig. 2, the proposed observer is described by a cascaded composition, where the attitude observer estimates are fed into the position observer to rotate the specific force readings to Earth frame. In this section the attitude and the position observers are detailed, and the associated properties are derived. Namely, the exponential convergence of the attitude and position estimation errors to the origin is evidenced, and it is shown that the attitude and position observer equations can be expressed as explicit functions of the IMU and GPS pseudorange measurements.

A. Attitude Observer

The attitude observer considered in this section estimates the rotation matrix by exploiting the angular velocity measurements (1), and *i)* the pseudorange measurements (3) provided by multiple GPS receivers installed onboard the vehicle, or *ii)* vector observations as proposed in [23]. The attitude observer estimates the orientation of the rigid body by computing the kinematics

$$\dot{\hat{\mathcal{R}}} = \hat{\mathcal{R}}(\hat{\boldsymbol{\omega}})_\times,$$

where $\hat{\mathcal{R}}$ is the estimated attitude and $\hat{\boldsymbol{\omega}}$ is the feedback term constructed to compensate for the attitude estimation error.

The architecture of the GPS based attitude observer is similar to that of the vector based attitude observer derived in [23], and further insight on the observer derivation can be found therein. The positions of two GPS receivers in body coordinates, ${}^B\bar{\mathbf{p}}_i$ and ${}^B\bar{\mathbf{p}}_1$, are subtracted to define the vector

$${}^B\bar{\mathbf{x}}_i := {}^B\bar{\mathbf{p}}_{i+1} - {}^B\bar{\mathbf{p}}_1, \tag{4}$$

which is known in body frame coordinates. Applying this operation to all the receivers produces $\mathbf{X} := \begin{bmatrix} {}^B\bar{\mathbf{x}}_1 & {}^B\bar{\mathbf{x}}_2 & \ldots & {}^B\bar{\mathbf{x}}_{r-1} \end{bmatrix} \in \mathrm{M}(3, r-1)$. Define the linear combination of the body vectors as

$${}^B\mathbf{y}_j := \sum_{i=1}^{r-1} b_{ij}\, {}^B\mathbf{x}_i \quad \Leftrightarrow \quad \mathbf{Y}_X = \mathbf{X}\mathbf{B}_X, \tag{5}$$

where $\mathbf{B}_X := [b_{ij}] \in \mathrm{M}(r-1)$ is invertible by construction and $\mathbf{Y}_X := \begin{bmatrix} {}^B\mathbf{y}_1 & \dots & {}^B\mathbf{y}_{r-1} \end{bmatrix} \in \mathrm{M}(3, r-1)$. The nominal and the estimated coordinates of the transformed body vectors in Earth frame are given by ${}^E\bar{\mathbf{Y}}_X := \bar{\mathcal{R}}\mathbf{Y}_X$ and ${}^E\hat{\mathbf{Y}}_X := \hat{\mathcal{R}}\mathbf{Y}_X$, respectively.

Some rotational degrees of freedom are unobservable if the vectors (4) are all collinear, and the following necessary condition is assumed.

Assumption 1: There are at least two noncollinear vectors ${}^B\bar{\mathbf{x}}_i$.

The transformation $\mathbf{B}_X$ is defined such that $\mathbf{Y}_X\mathbf{Y}_X' = \mathbf{I}$, to shape uniformly the directionality introduced by the vector readings. The desired $\mathbf{B}_X$ exists if Assumption 1 is satisfied, see [23, Appendix A] for a discussion on the subject.

The attitude observer is described by

$$\dot{\hat{\mathcal{R}}} = \hat{\mathcal{R}}(\hat{\boldsymbol{\omega}})_\times, \quad \hat{\boldsymbol{\omega}} = \hat{\mathcal{R}}'{}^E\bar{\mathbf{Y}}_X{}^E\hat{\mathbf{Y}}_X'\hat{\mathcal{R}}\left(\boldsymbol{\omega}_r - \hat{\mathbf{b}}_\omega\right) - k_\omega \mathbf{s}_\omega,$$

$$\dot{\hat{\mathbf{b}}}_\omega = k_b \mathbf{s}_\omega, \quad \mathbf{s}_\omega = \hat{\mathcal{R}}'\sum_{i=1}^{n}({}^E\bar{\mathbf{Y}}_X\mathbf{e}_i)\times({}^E\hat{\mathbf{Y}}_X\mathbf{e}_i), \tag{6}$$

where ${}^E\hat{\mathbf{Y}}_X$ and ${}^E\bar{\mathbf{Y}}_X$ are given by the observer estimates and the pseudorange measurements, respectively, as shown in the following proposition.

Proposition 1: Assume that the position fix $({}^E\bar{\mathbf{p}}, b_c)$ satisfying the pseudorange measurements (3) for all $i = 1..s$ is unique. The attitude observer dynamics (6) are a function of the sensor measurements and observer estimates, where

$${}^E\bar{\mathbf{Y}}_X = -\begin{bmatrix} \mathbf{f}_p(\boldsymbol{\rho}_2) - \mathbf{f}_p(\boldsymbol{\rho}_1) & \dots & \mathbf{f}_p(\boldsymbol{\rho}_r) - \mathbf{f}_p(\boldsymbol{\rho}_1)\end{bmatrix}\mathbf{B}_X,$$

${}^E\hat{\mathbf{Y}}_X = \hat{\mathcal{R}}\mathbf{X}\mathbf{B}_X$, $\boldsymbol{\rho}_j := \begin{bmatrix}\rho_{1j} & \dots & \rho_{mj}\end{bmatrix}$ is the vector of pseudoranges measured by receiver j, $\boldsymbol{\rho} := \boldsymbol{\rho}_1$, and the function $\mathbf{f}_p(\boldsymbol{\rho}_j)$ is given by

$$\mathbf{f}_p(\boldsymbol{\rho}_j) := \frac{1}{2}({}^E\mathbf{U}'\mathbf{W}_{Sj}{}^E\mathbf{U})^{-1}{}^E\mathbf{U}'\mathbf{W}_{Sj}\mathbf{b}_{Sj}, \tag{7}$$

which encompasses matrices described by the pseudoranges measurements and satellite's positions as follows

$$\begin{aligned}
{}^E\mathbf{U} &:= \begin{bmatrix}{}^E\bar{\mathbf{p}}_{S2}' - {}^E\bar{\mathbf{p}}_{S1}' & \dots & {}^E\bar{\mathbf{p}}_{Ss}' - {}^E\bar{\mathbf{p}}_{S1}'\end{bmatrix}',\\
\mathbf{W}_{S\,j} &:= 4\boldsymbol{\Delta}_{S\,j}(4\boldsymbol{\Delta}_{S\,j}'\boldsymbol{\Delta}_{S\,j} - 1)^{-1}\boldsymbol{\Delta}_{S\,j}' - \mathbf{I}_{(s-1)\times(s-1)},\\
\boldsymbol{\Delta}_{Sj} &:= \begin{bmatrix}\rho_{2j} - \rho_{1j} & \dots & \rho_{sj} - \rho_{1j}\end{bmatrix}',\\
\mathbf{b}_{S\,j} &= \begin{bmatrix}\rho_{2j}^2 - \rho_{1j}^2 - \left(\|{}^E\bar{\mathbf{p}}_{S\,2}\|^2 - \|{}^E\bar{\mathbf{p}}_{S\,1}\|^2\right)\\ \vdots \\ \rho_{s\,j}^2 - \rho_{1\,j}^2 - \left(\|{}^E\bar{\mathbf{p}}_{S\,s}\|^2 - \|{}^E\bar{\mathbf{p}}_{S\,1}\|^2\right)\end{bmatrix}.
\end{aligned} \tag{8}$$

Proof: The formulation for ${}^E\hat{\mathbf{Y}}_X$ is immediate from (5), and ${}^E\bar{\mathbf{Y}}_X$ is obtained by noting that ${}^E\bar{\mathbf{Y}}_X = \begin{bmatrix}{}^E\bar{\mathbf{p}}_2 - {}^E\bar{\mathbf{p}}_1 & \dots & {}^E\bar{\mathbf{p}}_r - {}^E\bar{\mathbf{p}}_1\end{bmatrix}\mathbf{B}_X$ and using the derivation of $\mathbf{f}_p(\boldsymbol{\rho}_j)$ presented in the Appendix. ∎

The resulting stability and convergence properties of the attitude observer are formulated by defining the attitude estimation error $\tilde{\mathcal{R}} := \hat{\mathcal{R}}'\bar{\mathcal{R}}$. The Euler angle-axis parametrization of $\tilde{\mathcal{R}}$ is described by the rotation vector $\boldsymbol{\lambda} \in \mathrm{S}(2)$ and by the rotation angle $\theta \in \begin{bmatrix}0 & \pi\end{bmatrix}$, and yields the Direct Cosine Matrix (DCM) formulation $\tilde{\mathcal{R}} = \mathrm{rot}(\theta, \boldsymbol{\lambda}) := \cos(\theta)\mathbf{I} + \sin(\theta)(\boldsymbol{\lambda})_\times + (1-\cos(\theta))\boldsymbol{\lambda}\boldsymbol{\lambda}'$, see [17] for details.

The properties of the observer are presented separately for the case of unbiased and biased angular measurements, since the former presents stronger convergence properties. For details, the reader is referred to the proofs in [23].

Theorem 2 (Unbiased Velocity Measurements): Let $\bar{\mathbf{b}}_\omega = 0$. Under Assumption 1, the closed-loop error kinematics of the attitude observer are given by

$$\dot{\tilde{\mathcal{R}}} = -k_\omega\tilde{\mathcal{R}}(\tilde{\mathcal{R}} - \tilde{\mathcal{R}}'). \tag{9}$$

The equilibrium point $\tilde{\mathcal{R}} = \mathbf{I}$ is exponentially stable, with region of attraction $R_A = \{\tilde{\mathcal{R}} \in \mathrm{SO}(3) : \mathrm{tr}(\mathbf{I} - \tilde{\mathcal{R}}) < 4\}$ $= \{\tilde{\mathcal{R}} \in \mathrm{SO}(3) : \tilde{\mathcal{R}} = \mathrm{rot}(\theta, \pi), |\theta| < \pi\}$ and for any initial condition $\tilde{\mathcal{R}}(t_0) \in R_A$, the emanating trajectory satisfies

$$\|\tilde{\mathcal{R}}(t) - \mathbf{I}\| \le c_{\mathcal{R}}\|\tilde{\mathcal{R}}(t_0) - \mathbf{I}\|e^{-\frac{1}{2}\gamma_{\mathcal{R}}(t-t_0)}, \tag{10}$$

where $c_{\mathcal{R}} = 1$ and $\gamma_{\mathcal{R}} = 2k_\omega(1 + \cos(\theta(t_0)))$.

Theorem 3 (Biased Velocity Measurements): Let $\bar{\mathbf{b}}_\omega \neq 0$. Under Assumption 1, the closed loop dynamics are given by

$$\dot{\tilde{\mathcal{R}}} = -k_\omega\tilde{\mathcal{R}}(\tilde{\mathcal{R}} - \tilde{\mathcal{R}}') + \tilde{\mathcal{R}}(\tilde{\mathbf{b}}_\omega)_\times,\ \dot{\tilde{\mathbf{b}}}_\omega = -k_b(\tilde{\mathcal{R}} - \tilde{\mathcal{R}}')_\otimes, \tag{11}$$

where $(\cdot)_\otimes$ is the unskew operator such that $((\mathbf{w})_\times)_\otimes = \mathbf{w}, \mathbf{w} \in \mathbb{R}^3$. Given the feedback gain $k_b > \frac{\tilde{b}_{0\,\max}^2}{4(1+\cos(\theta_{0\,\max}))}$ where $\theta_{0\,\max}$ and $\tilde{b}_{0\,\max}$ represent the initial estimation errors bounds

$$\theta(t_0) \le \theta_{0\,\max} < \pi, \quad \|\tilde{\mathbf{b}}_\omega(t_0)\| \le \tilde{b}_{0\,\max}, \tag{12}$$

the origin $(\tilde{\mathcal{R}}, \tilde{\mathbf{b}}_\omega) = (\mathbf{I}, 0)$ is exponentially stable, uniformly in the set defined by (12). That is, let $\mathbf{x}_{\mathcal{R}} := \left(\tilde{\mathcal{R}} - \mathbf{I}, \tilde{\mathbf{b}}_\omega\right)$, there exists $c_b, \gamma_b > 0$ independent of $\mathbf{x}_{\mathcal{R}}(t_0)$ such that the trajectories of the system satisfy

$$\|\mathbf{x}_{\mathcal{R}}(t)\| \le c_b e^{-\frac{1}{2}\gamma_{b_\omega}(t-t_0)}\|\mathbf{x}_{\mathcal{R}}(t_0)\|. \tag{13}$$

Bounds for the exponential convergence parameters c_b and γ_{b_ω} are given by the properties of parameterized linear time-varying systems presented in [16], for details and discussion of the results for the present observer see [23, Corollary 9].

The attitude observer based on vector observations is detailed in [23] and is characterized by the dynamics, and the convergence and stability properties described in Theorem 2 and Theorem 3.

B. Position Observer

This section derives the position observer based on the IMU and GPS readings, and on the attitude observer estimates. The position and velocity estimates are described by

$${}^E\dot{\hat{\mathbf{p}}} = {}^E\hat{\mathbf{v}} + \mathbf{s}_p, \quad {}^E\dot{\hat{\mathbf{v}}} = {}^E\hat{\mathbf{a}} + \mathbf{s}_v, \tag{14}$$

where $\mathbf{s}_p$ and $\mathbf{s}_v$ are feedback terms, the estimate of the acceleration in Earth coordinates is given by

$${}^E\hat{\mathbf{a}} = \hat{\mathcal{R}}\mathbf{a}_r + {}^E\bar{\mathbf{g}}, \tag{15}$$

and the gravity representation in Earth coordinates ${}^E\bar{\mathbf{g}}$ is known. As shown in the block diagram of Fig. 2, the position observer uses the attitude estimate to rotate the accelerometer measurements $\mathbf{a}_r$ to the Earth frame. Consequently, the attitude estimation error $\tilde{\mathcal{R}}$ will affect the convergence and stability properties of the position observer.

Defining the position and velocity estimation errors ${}^E\tilde{\mathbf{p}} := {}^E\hat{\mathbf{p}} - {}^E\bar{\mathbf{p}}$, ${}^E\tilde{\mathbf{v}} := {}^E\hat{\mathbf{v}} - {}^E\bar{\mathbf{v}}$, the derivation of the feedback terms $\mathbf{s}_p$ and $\mathbf{s}_v$ is motivated by the Lyapunov function

$$V_p := \frac{\alpha_p}{2}\|{}^E\tilde{\mathbf{p}}\|^2 + \frac{\alpha_v}{2}\|{}^E\tilde{\mathbf{v}}\|^2. \tag{16}$$

The Lyapunov function time derivative is described by $\dot{V}_p = \alpha_p {}^E\tilde{\mathbf{p}}'({}^E\tilde{\mathbf{v}} + \mathbf{s}_p) + \alpha_v {}^E\tilde{\mathbf{v}}'(\mathbf{u}_g + \mathbf{s}_v)$, where $\mathbf{u}_g := \bar{\mathcal{R}}(\tilde{\mathcal{R}}' - \mathbf{I})\bar{\mathcal{R}}'({}^E\bar{\mathbf{a}} - {}^E\bar{\mathbf{g}})$. The feedback terms are defined as

$$\mathbf{s}_p := -k_p {}^E\tilde{\mathbf{p}}, \quad \mathbf{s}_v := -k_v {}^E\tilde{\mathbf{p}}, \tag{17}$$

where $k_p, k_v > 0$, and choosing $\alpha_v = \frac{\alpha_p}{k_v}$ produces

$$\dot{V}_p = -\alpha_p k_p \|{}^E\tilde{\mathbf{p}}\|^2 + \frac{\alpha_p}{k_v} {}^E\tilde{\mathbf{v}}'\mathbf{u}_g. \tag{18}$$

which is sign indefinite due to the second term. The term $\mathbf{u}_g$ is the compensation error generated by rotating the accelerometer readings to Earth frame using the estimated attitude. In particular, if $\mathbf{u}_g = 0$, then $\dot{V}_p$ is negative definite and the stability properties of the position observer can be derived using Lyapunov stability theory. However, for $\mathbf{u}_g \neq 0$, the convergence properties of the position observer are influenced by the convergence properties of the attitude observer.

The position and velocity error dynamics are described by

$$\begin{aligned} {}^E\dot{\tilde{\mathbf{p}}} &= -k_p {}^E\tilde{\mathbf{p}} + {}^E\tilde{\mathbf{v}}, \\ {}^E\dot{\tilde{\mathbf{v}}} &= -k_v {}^E\tilde{\mathbf{p}} + \bar{\mathcal{R}}(\tilde{\mathcal{R}}' - \mathbf{I})\bar{\mathcal{R}}'({}^E\bar{\mathbf{a}} - {}^E\bar{\mathbf{g}}), \end{aligned} \tag{19}$$

which can be modeled as an autonomous system with an input $\mathbf{u}_g$. In this work, the stability of the position observer is obtained by using input-to-state stability theory [13], [20]. To that effect, it is assumed that the following condition for the rigid body acceleration is verified.

Assumption 2: For any $\gamma_g > 0$, there exists c_g such that the acceleration of the rigid body satisfies

$$\|{}^E\bar{\mathbf{a}}(t) - {}^E\bar{\mathbf{g}}\| \leq c_g e^{\gamma_g(t-t_0)}, \text{for all } t > t_0. \tag{20}$$

The conditions of Assumption 2 guarantee that the convergence of the attitude estimation error $(\mathbf{I} - \tilde{\mathcal{R}})$ dominates the acceleration term $({}^E\bar{\mathbf{a}} - {}^E\bar{\mathbf{g}})$ in $\mathbf{u}_g$ as $t \to \infty$. Interestingly enough, unbounded accelerations such as those that grow polynomially with time satisfy Assumption 2, which therefore poses a weak limitation for most practical applications.

We are now ready to present the stability and convergence properties of the cascaded attitude and position observers. As before, the properties are derived separately for unbiased and biased angular rate measurements.

Theorem 4 (Unbiased Velocity Measurements): Under Assumptions 1 and 2, the equilibrium point $(\tilde{\mathcal{R}}, {}^E\tilde{\mathbf{p}}, {}^E\tilde{\mathbf{v}}) = (\mathbf{I}, \mathbf{0}, \mathbf{0})$ of the system (9,19) is exponentially stable with region of attraction given by

$$\begin{aligned} R_A &= \{(\tilde{\mathcal{R}}, {}^E\tilde{\mathbf{p}}, {}^E\tilde{\mathbf{v}}) \in \mathrm{SE}(3) \times \mathbb{R}^3 : \mathrm{tr}(\mathbf{I} - \tilde{\mathcal{R}}) < 4\} \\ &= \{(\mathrm{rot}(\theta, \boldsymbol{\lambda}), {}^E\tilde{\mathbf{p}}, {}^E\tilde{\mathbf{v}}) \in \mathrm{SE}(3) \times \mathbb{R}^3 : |\theta| < \pi\}. \end{aligned}$$

Proof: The stability and convergence of the position and attitude errors are shown by analyzing (9) and (19) as a cascaded system. The position and velocity error dynamics expressed in (19) are rewritten as

$$\dot{\mathbf{x}}_p = \mathbf{A}_p\mathbf{x}_p + \mathbf{B}_p\mathbf{u}_g, \tag{21}$$

where $\mathbf{x}_p := \begin{bmatrix} {}^E\tilde{\mathbf{p}}' & {}^E\tilde{\mathbf{v}}' \end{bmatrix}'$, $\mathbf{A}_p := \begin{bmatrix} -k_p\mathbf{I} & \mathbf{I} \\ -k_v\mathbf{I} & \mathbf{0} \end{bmatrix}$, $\mathbf{B}_p := \begin{bmatrix} \mathbf{0} \\ \mathbf{I} \end{bmatrix}$. To derive the stability and convergence properties of the cascaded system, it is first shown that the system represented by (21) is Input to State Stable (ISS). It is a simple exercise to verify that $\mathbf{A}_p$ is Hurwitz and, by the properties of linear systems [13], the system (21) is ISS.

The exponential convergence of the state $(\tilde{\mathcal{R}}, {}^E\tilde{\mathbf{p}}, {}^E\tilde{\mathbf{v}})$ is obtained by the bounds on the solution of (21) and the exponential convergence of $\mathbf{u}_g$. The derivation is presented here for the sake of clarity and to provide explicit convergence bounds. Using $\|\mathbf{u}_g\| \leq \|\bar{\mathcal{R}}(\tilde{\mathcal{R}}' - \mathbf{I})\|\|\bar{\mathcal{R}}'({}^E\bar{\mathbf{a}} - {}^E\bar{\mathbf{g}})\| = \|\tilde{\mathcal{R}} - \mathbf{I}\|\|{}^E\bar{\mathbf{a}} - {}^E\bar{\mathbf{g}}\|$, the exponential convergence of the attitude observer error (10), and Assumption 2, a exponential bound for the input is obtained

$$\|\mathbf{u}_g(t)\| \leq c_e e^{-\gamma_e(t-t_0)}\|\tilde{\mathcal{R}}(t_0) - \mathbf{I}\|, \tag{22}$$

where $c_e := c_{\mathcal{R}}c_g$ and $\gamma_e := \gamma_{\mathcal{R}} - \gamma_g$. Choosing γ_g small enough, the exponential rate satisfies $\gamma_e > 0$. Therefore $\|\mathbf{u}_g\| \to 0$ and, by the ISS property of (19), $\|{}^E\tilde{\mathbf{p}}\| \to 0$ and $\|{}^E\tilde{\mathbf{v}}\| \to 0$ as $t \to \infty$.

To see that the origin of (9,19) is in fact exponentially stable, note that the solution of the LTI system (21) satisfies

$$\|\mathbf{x}_p(t)\| \leq c_a e^{-\gamma_a(t-t_0)}\|\mathbf{x}_p(t_0)\| + \int_{t_0}^{t} c_a e^{-\gamma_a(t-\tau)}\|\mathbf{B}_p\|\|\mathbf{u}_g(\tau)\|d\tau$$

where the stability of the origin implies that there exists c_a and $\gamma_a > 0$ such that $\|e^{\mathbf{A}_p t}\| \leq c_a e^{-\gamma_a t}$ [13]. Applying (22), solving the integral and using the inequalities $\frac{e^{-\gamma_e(t-t_0)} - e^{-\gamma_a(t-t_0)}}{\gamma_a - \gamma_e} \leq \frac{e^{-\gamma_{\min}(t-t_0)}}{|\gamma_a - \gamma_e|}$, and $e^{-\gamma_a(t-t_0)} \leq e^{-\gamma_{\min}(t-t_0)}$, where $\gamma_{\min} := \min(\gamma_e, \gamma_a)$, produces

$$\|\mathbf{x}_p(t)\| \leq c_a e^{-\gamma_{\min}(t-t_0)}(\|\mathbf{x}_p(t_0)\| + \frac{c_e\|\mathbf{B}_p\|}{|\gamma_a - \gamma_e|}\|\tilde{\mathcal{R}}(t_0) - \mathbf{I}\|).$$

Defining the full attitude and position estimation error state $\mathbf{x}_f := \left(\tilde{\mathcal{R}} - \mathbf{I}, \mathbf{x}_p\right) = (\tilde{\mathcal{R}} - \mathbf{I}, {}^E\tilde{\mathbf{p}}, {}^E\tilde{\mathbf{v}})$, using (10), $\|\mathbf{x}_f\| \leq \|\mathbf{x}_p\| + \|\tilde{\mathcal{R}} - \mathbf{I}\|$, $\|\mathbf{x}_p\| \leq \|\mathbf{x}_f\|$, $\|\tilde{\mathcal{R}} - \mathbf{I}\| \leq \|\mathbf{x}_f\|$, and $\gamma_e < \gamma_{\mathcal{R}}$ results in the exponential bound

$$\|\mathbf{x}_f(t)\| \leq c_{\max} e^{-\gamma_{\min}(t-t_0)}\|\mathbf{x}_f(t_0)\|,$$

where $c_{\max} := 2\max(c_a, \frac{c_a c_e\|\mathbf{B}_p\|}{|\gamma_a - \gamma_e|} + k_{\mathcal{R}})$. ■

Following the proof of Theorem 4, it is possible to show that if (20) is verified for some $c_g, \gamma_g > 0$, i.e. if the acceleration grows exponentially with time, then there is a sufficiently high gain k_ω such that the origin is exponentially stable for all $\theta_0 \leq \theta_{\max} < 0$.

The stability and convergence result for position and attitude estimation with biased angular velocity measurements is presented next.

Theorem 5 (Biased Angular Velocity Measurements): Consider the feedback gain $k_b > \frac{\tilde{b}_{0\max}^2}{4(1+\cos(\theta_{0\max}))}$. Under Assumptions 1 and 2, the equilibrium point $(\tilde{\mathcal{R}}, \tilde{\mathbf{b}}_\omega, {}^E\tilde{\mathbf{p}}, {}^E\tilde{\mathbf{v}}) = (\mathbf{I}, \mathbf{0}, \mathbf{0}, \mathbf{0})$ of the system (11,19) is exponentially stable, uniformly in the set defined by (12).

Proof: By Theorem 3, the attitude observer error $\mathbf{x}_{\mathcal{R}}$ is bounded by (13). Using $\|\tilde{\mathcal{R}} - \mathbf{I}\| \leq \|\mathbf{x}_{\mathcal{R}}\|$, the input of the ISS system (19) is bounded by

$$\|\mathbf{u}_g(t)\| \leq c_{be} e^{-\gamma_{be}(t-t_0)}\|\mathbf{x}_{\mathcal{R}}(t_0)\|, \tag{23}$$

where $c_{be} := c_b c_g$ and $\gamma_{be} := \frac{1}{2}\gamma_b - \gamma_g$. Repeating the algebraic manipulations of the proof of Theorem 4 produces

$$\|\mathbf{x}_{bf}(t)\| \leq c_{\max} e^{-\gamma_{\min}(t-t_0)} \|\mathbf{x}_{bf}(t_0)\|,$$

where $\mathbf{x}_{bf} := (\mathbf{x}_{\mathcal{R}}, \mathbf{x}_p) = (\tilde{\mathcal{R}} - \mathbf{I}, \tilde{\mathbf{b}}_\omega, {}^E\tilde{\mathbf{p}}, {}^E\tilde{\mathbf{v}})$ is the full attitude and position estimation error state, $\gamma_{\min} := \min(\gamma_{be}, \gamma_a)$ and $c_{\max} := 2\max(c_a, \frac{c_a c_{be}\|\mathbf{B}_p\|}{|\gamma_a - \gamma_{be}|} + k_b)$. ∎

As shown in the next proposition, the position and velocity estimation errors are bounded in the presence of accelerometer disturbances.

Proposition 6 (Accelerometer Noise): Let the accelerometer measurements be corrupted by bounded noise

$$\mathbf{a}_r = {}^B\bar{\mathbf{a}} - {}^B\bar{\mathbf{g}} + \mathbf{n}_a,$$

where $\mathbf{n}_a \in \mathbb{R}^3$, $\|\mathbf{n}_a\| \leq n_{max}$. Then, the estimation errors ${}^E\tilde{\mathbf{p}}$ and ${}^E\tilde{\mathbf{v}}$ are bounded.

Proof: The result stems directly from the ISS properties of the position observer. The position estimation error dynamics are given by

$${}^E\dot{\tilde{\mathbf{p}}} = -k_p {}^E\tilde{\mathbf{p}} + {}^E\tilde{\mathbf{v}}, \quad {}^E\dot{\tilde{\mathbf{v}}} = -k_v {}^E\tilde{\mathbf{p}} + \mathbf{u}_g + \hat{\mathcal{R}}\mathbf{n}_a.$$

Using the triangle inequality $\|\mathbf{u}_g + \hat{\mathcal{R}}\mathbf{n}_a\| \leq \|\mathbf{u}_g\| + \|\hat{\mathcal{R}}\mathbf{n}_a\|$ and $\|\hat{\mathcal{R}}\mathbf{n}_a\| = \|\mathbf{n}_a\|$, the position solution is bounded by $\|\mathbf{x}_p(t)\| \leq c_a e^{-\gamma_a(t-t_0)}\|\mathbf{x}_p(t_0)\| + \int_{t_0}^{t} c_a e^{-\gamma_a(t-\tau)}\|\mathbf{B}_p\|(\|\mathbf{u}_g(\tau)\| + \|\mathbf{n}_a(\tau)\|)d\tau$. Taking the bound $\int_{t_0}^{t} e^{-\gamma_a(t-\tau)}\|\mathbf{n}_a(\tau)\|d\tau \leq \frac{n_{\max}}{\gamma_a}$ shows that $\limsup_{t\to\infty}(\|\mathbf{x}_p(t)\|) \leq \frac{c_a}{\gamma_a}\|\mathbf{B}_p\| n_{\max}$. ∎

Interestingly enough, the derived position and velocity observer equations (14) can be written as a function of the observer estimates and of the sensor measurements, as shown in the next proposition.

Proposition 7: Assume that the position fix $({}^E\bar{\mathbf{p}}, b_c)$ satisfying the pseudorange measurements (3) for all $i = 1..s$ is unique. The dynamics of the position and velocity estimates are a function of the sensor measurements and observer estimates

$$\begin{aligned} {}^E\dot{\hat{\mathbf{p}}} &:= -k_p\left({}^E\hat{\mathbf{p}} + \mathbf{f}_p(\boldsymbol{\rho})\right) + {}^E\hat{\mathbf{v}}, \\ {}^E\dot{\hat{\mathbf{v}}} &:= -k_v\left({}^E\hat{\mathbf{p}} + \mathbf{f}_p(\boldsymbol{\rho})\right) + \hat{\mathcal{R}}\mathbf{a}_r + {}^E\bar{\mathbf{g}}. \end{aligned} \tag{24}$$

Proof: The formulation (24) is obtained by algebraic manipulation of (14) and (17), and by writing the nominal position term in ${}^E\tilde{\mathbf{p}} = {}^E\hat{\mathbf{p}} - {}^E\bar{\mathbf{p}}$ as a solution of the pseudorange measurements. The details of the derivation are presented in the Appendix. ∎

IV. SIMULATIONS

In this section, simulation results for the proposed position and attitude observer are presented. The GPS based attitude observer was simulated using GPS receivers placed at ${}^B\mathbf{p}_1 = \left[\begin{smallmatrix}0\\0\\0\end{smallmatrix}\right]$ m, ${}^B\mathbf{p}_2 = \left[\begin{smallmatrix}1.5\\0\\0\end{smallmatrix}\right]$ m, ${}^B\mathbf{p}_3 = \left[\begin{smallmatrix}0\\2\\0\end{smallmatrix}\right]$ m. The satellites configuration is described by ${}^E\mathbf{p}_{S1} = \left[\begin{smallmatrix}0\\0\\-20\times10^6\end{smallmatrix}\right]$ m, ${}^E\mathbf{p}_{S2} = \left[\begin{smallmatrix}44\times10^6\\0\\-20\times10^6\end{smallmatrix}\right]$ m, ${}^E\mathbf{p}_{S3} = \left[\begin{smallmatrix}0\\44\times10^6\\-20\times10^6\end{smallmatrix}\right]$ m, ${}^E\mathbf{p}_{S4} = \left[\begin{smallmatrix}0\\0\\0\end{smallmatrix}\right]$ m, ${}^E\mathbf{p}_{S5} = \left[\begin{smallmatrix}10^3\\0\\0\end{smallmatrix}\right]$ m where $\mathbf{p}_{S4}$ and $\mathbf{p}_{S5}$ are the coordinates of pseudo-satellites installed at ground level. The clock bias, expressed in distance, is $b_c = 10^5$ m.

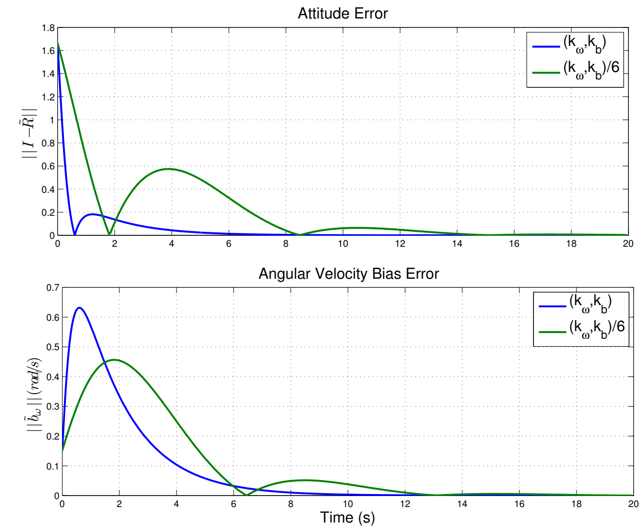

Fig. 3. Attitude and Bias Estimation.

The feedback gains are given by $k_\omega = 2, k_b = 1, k_p = 2, k_v = \frac{1}{2}$ and the rigid body trajectory is computed using oscillatory angular rates and accelerations of 1 Hz. The initial estimation errors are ${}^E\tilde{\mathbf{p}}(t_0) = \left[\begin{smallmatrix}-10\\-10\\20\end{smallmatrix}\right]$ m, ${}^E\tilde{\mathbf{v}}(t_0) = \left[\begin{smallmatrix}1\\1\\1\end{smallmatrix}\right]$ m/s, $\theta(t_0) = \frac{72\pi}{180}$ rad. The rate gyro bias is identical on each rate gyro channel $\bar{\mathbf{b}}_\omega = \left[\begin{smallmatrix}5\\5\\5\end{smallmatrix}\right]\frac{\pi}{180}$ rad/s, and the initial bias estimate is $\hat{\mathbf{b}}_\omega(t_0) = \mathbf{0}$ rad/s. The bounds (12) are defined by $\theta_{0\max} = \frac{135\pi}{180}$ rad, $\tilde{b}_{0\max} = \frac{5\sqrt{3}\pi}{180}$ rad/s.

The attitude and position estimation errors converge to the origin, as illustrated in Fig. 3 and Fig. 4. Reducing the attitude feedback gains k_ω and k_b, the convergence rate of the attitude and position estimates is slower, as expected.

Considering that the accelerometer readings are corrupted by a Gaussian white noise $\mathbf{n}_a$ with standard deviation $\sigma_a = 0.1\mathbf{I}\ m/s^2$ and bounded by $\|\mathbf{n}_a\| \leq n_{\max} = 0.3\ m/s^2$, the position and velocity estimation errors converge to a neighborhood of the origin, as shown in Fig. 4. The norm of the specific acceleration compensation term $\mathbf{u}_g$ converges to a nonzero value below $n_{\max}$, as expected.

The simulation results for the attitude observer based on vector observations are similar to those presented for the GPS based observer, given that the error dynamics are identical.

V. CONCLUSIONS

A nonlinear observer for attitude and position estimation on SE(3) exploiting GPS and IMU data was derived. The resulting navigation system structure was described by a cascade of the attitude and position observers, yielding exponential convergence of the estimation errors to the origin and stability in the presence of bounded accelerometer noise. Simulation results depicted the convergence properties of the estimation errors. Future work will focus on the discrete time implementation of the algorithm for practical applications.

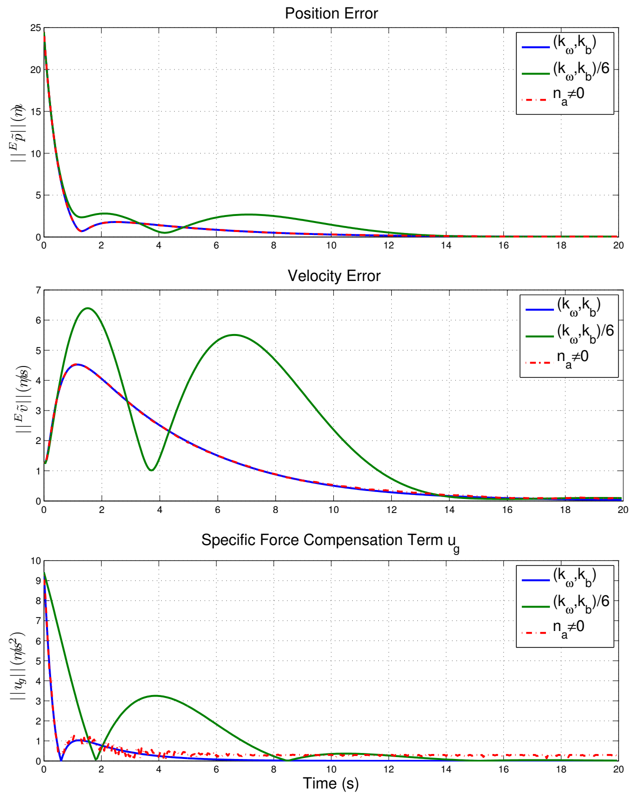

Fig. 4. Position and Velocity Estimation.

APPENDIX

In this section, the solution to the GPS receiver position given the pseudorange measurements is derived. The present approach builds on the geometric method presented in [8] for $s > 4$ satellites, and is presented for the sake of clarity. Consider two pseudorange measurements (3) obtained by receiver j with respect to satellites i and 1, that is ρ_{ij} and ρ_{1j}, respectively. Squaring and subtracting the pseudoranges yields $\mathbf{A}_{S\,j}\begin{bmatrix}{}^E\bar{\mathbf{p}}_j \\ b_c\end{bmatrix} = \mathbf{b}_{S\,j}$ where $\mathbf{A}_{S\,j} := 2\begin{bmatrix}-{}^E\mathbf{U} & \boldsymbol{\Delta}_{S\,j}\end{bmatrix}$ and $\mathbf{b}_{S\,j}$ is defined in (8). A solution is given by the pseudoinverse $\begin{bmatrix}{}^E\bar{\mathbf{p}}_j \\ b_c\end{bmatrix} = (\mathbf{A}'_{S\,j}\mathbf{A}_{S\,j})^{-1}\mathbf{A}'_{S\,j}\mathbf{b}_{S\,j}$ which, by algebraic manipulation and using the properties of the block matrix inverse, produces

$$ {}^E\bar{\mathbf{p}}_j = -\frac{({}^E\mathbf{U}'\mathbf{W}_{Sj}{}^E\mathbf{U})^{-1}{}^E\mathbf{U}'\mathbf{W}_{Sj}\mathbf{b}_{Sj}}{2} = -\mathbf{f}_p(\boldsymbol{\rho}_j). \qquad (25) $$

The conditions for existence and uniqueness of a position fix ${}^E\bar{\mathbf{p}}_j$ given the pseudorange measurements ρ_{ij} depend on the user-satellite geometry for $s = 4$ satellites [8], [15]. For $s \geq 5$, the solution is unique if the satellite geometry is nonplanar [1]. If a valid position fix ${}^E\bar{\mathbf{p}}_j$ exists then it satisfies (25), however if $\operatorname{rank}(\mathbf{A}_{S\,j}) < 4$ the solution for any nonplanar satellite configuration is given by [8, p.1024]

$$ \begin{bmatrix}{}^E\bar{\mathbf{p}}_j \\ b_c\end{bmatrix} = \mathbf{w}_{S\,j} + \alpha\mathbf{a}_\perp, \mathbf{w}_{S\,j} = \mathbf{A}^{*'}_{S\,j}(\mathbf{A}^*_{S\,j}\mathbf{A}^{*'}_{S\,j})^{-1}\mathbf{A}^*_{S\,j}\mathbf{b}_{S\,j}, $$

where $\mathbf{A}^*_{S\,j} \in \mathrm{M}(3,4)$ is obtained by selecting the linearly independent lines of $\mathbf{A}_{S\,j}$, $\mathbf{a}_\perp \in \mathbb{R}^4$ describes the null space of $\mathbf{A}_{S\,j}$, i.e. $\mathbf{A}_{S\,j}\mathbf{a}_\perp = 0$, and the coefficient α is the solution of the quadratic equation $\alpha^2\mathbf{w}'_a\mathbf{Z}\mathbf{w}_a + 2\alpha\mathbf{w}'_a\mathbf{Z}\mathbf{a}_\perp + \mathbf{a}'_\perp\mathbf{Z}\mathbf{a}_\perp = 0$, $\mathbf{w}_a = \mathbf{w}_{S\,j} - \begin{bmatrix}{}^E\mathbf{p}'_{S1} & \rho_{1j}\end{bmatrix}'$, $\mathbf{Z} = \operatorname{diag}(1,1,1,-1)$, which uniquely satisfies the pseudorange measurements ρ_{ij}.

REFERENCES

[1] J. Abel and J. Chaffee. Existence and Uniqueness of GPS Solutions. *IEEE Transactions on Aerospace and Electronic Systems*, 27(6):952–956, Nov. 1991.

[2] J.L. Awange and E.W. Grafarend. Algebraic Solution of GPS Pseudo-Ranging Equations. *GPS Solutions*, 5(4):20–32, April 2002.

[3] G. Baldwin, R. Mahony, J. Trumpf, T. Hamel, and T. Cheviron. Complementary Filter Design on the Special Euclidean Group SE(3). In *Proceeding of the European Control Conference 2007*, Kos, Greece, July 2007.

[4] S. Bancroft. An Algebraic Solution of the GPS Equations. *Aerospace and Electronic Systems, IEEE Transactions on*, AES-21(1):56–59, Jan. 1985.

[5] S. P. Bhat and D. S. Bernstein. A Topological Obstruction to Continuous Global Stabilization of Rotational Motion and the Unwinding Phenomenon. *Systems and Control Letters*, 39(1):63–70, Jan. 2000.

[6] I. Biton, M. Koifman, and I. Y. Bar-Itzhack. Improved Direct Solution of the Global Positioning System Equation. *Journal of Guidance, Control, and Dynamics*, 21(1):45–49, Jan.-Feb. 1998.

[7] K. R. Britting. *Inertial Navigation Systems Analysis*. John Wiley & Sons Inc, 1972.

[8] J. Chaffee and J. Abel. On the Exact Solutions of Pseudorange Equations. *IEEE Transactions on Aerospace and Electronic Systems*, 30(4):1021–1030, Oct. 1994.

[9] N. Chaturvedi and N. McClamroch. Almost Global Attitude Stabilization of an Orbiting Satellite Including Gravity Gradient and Control Saturation Effects. In *Proceedings of the 2006 American Control Conference*, pages 1748–1753, Minnesota, USA, June 2006.

[10] J. L. Crassidis. Sigma-point Kalman Filtering for Integrated GPS and Inertial Navigation. *Aerospace and Electronic Systems, IEEE Transactions on*, 42(2):750–756, April 2006.

[11] M. S. Grewal, L. R. Weill, and A. P. Andrews. *Global Positioning Systems, Inertial Navigation, and Integration*. Wiley-Interscience, 2nd edition, 2007.

[12] L. Imsland, T.A. Johansen, T. I. Fossen, H.F. Grip, J.C. Kalkkuhl, and A. Suissa. Vehicle Velocity Estimation Using Nonlinear Observers. *Automatica*, 42:2091–2103, 2006.

[13] H. K. Khalil. *Nonlinear Systems*. Prentice Hall, 3rd edition, 2001.

[14] J. C. Kinsey and L. L. Whitcomb. Adaptive Identification on the Group of Rigid-Body Rotations and its Application to Underwater Vehicle Navigation. *IEEE Transactions on Robotics*, 23(1):124–136, Feb. 2007.

[15] J.L. Leva. An Alternative Closed-Form Solution to the GPS Pseudo-Range Equations. *Aerospace and Electronic Systems, IEEE Transactions on*, 32(4):1430–1439, Oct. 1996.

[16] A. Loría. Explicit Convergence Rates for MRAC-Type Systems. *Automatica*, 40(8):1465–1468, Aug. 2004.

[17] R. M. Murray, Z. Li, and S. S. Sastry. *A Mathematical Introduction to Robotic Manipulation*. CRC, 1994.

[18] H. Rehbinder and B. K. Ghosh. Pose Estimation Using Line-Based Dynamic Vision and Inertial Sensors. *IEEE Transactions on Automatic Control*, 48(2):186–199, Feb. 2003.

[19] S. Salcudean. A Globally Convergent Angular Velocity Observer for Rigid Body Motion. *IEEE Transactions on Automatic Control*, 36(12):1493–1497, 1991.

[20] E.D. Sontag. Input to State Stability: Basic Concepts and Results. In P. Nistri and G. Stefani, editors, *Nonlinear and Optimal Control Theory*, pages 163–220. Springer-Verlag, Berlin, 2007.

[21] S. Sukkarieh, E.M. Nebot, and H.F. Durrant-Whyte. A High Integrity IMU/GPS Navigation Loop for Autonomous Land Vehicle Applications. *Robotics and Automation, IEEE Transactions on*, 15(3):572–578, June 1999.

[22] J. Thienel and R. M. Sanner. A Coupled Nonlinear Spacecraft Attitude Controller and Observer With an Unknown Constant Gyro Bias and Gyro Noise. *IEEE Transactions on Automatic Control*, 48(11):2011–2015, Nov. 2003.

[23] J.F. Vasconcelos, C. Silvestre, and P. Oliveira. Nonlinear Observer for Rigid Body Attitude Estimation using Vector Observations. In *Proceedings of the 17th IFAC World Congress*, 2008.